JCEC
THE JOURNAL OF ENGINEERING AND EXACT SCIENCES

OPEN ACCESS

The Journal of Engineering and Exact Sciences – jCEC, Vol. 10 N. 01 (2024)
journal homepage: https://periodicos.ufv.br/jcec
eISSN: 2527-1075
ISSN: 2446-9416

Comparative study on perovskite solar cells using P_ZnO, Al_ZnO and In_ZnO as ETMs by SCAPS-1D

Article Info:
Article history: Received 2023-07-13 / Accepted 2023-12-26 / Available online 2024-01-05
doi: 10.18540/jcecvl10iss1pp17387

Meriem Kerara
Materials Science and Informatics Laboratory, Faculty of Science
University of Djelfa
Address: 17000, Djelfa, Algeria
E-mail: kerarameriem@gmail.com
Abdelkrim Naas
Materials Science and Informatics Laboratory, Faculty of Science
University of Djelfa
Address: 17000, Djelfa, Algeria
E-mail: abdelkrim_naas@yahoo.fr
Khalid Reggab
Materials Science and Informatics Laboratory, Faculty of Science
University of Djelfa
Address: 17000, Djelfa, Algeria
E-mail: khaledreggab@gmail.com

Abstract
This study uses the SCAPS 1D software to analyze solar cells with lead iodide perovskite ($CH_3NH_3PbI_3$) as the active material and three different types of ZnO doping: undoped (P_ZnO), aluminum-doped (Al_ZnO), and indium-doped (In_ZnO) as the electron transport layer (ETL). This study aims to investigate the effects of charge carrier density on the J-V characteristics and electrical properties (J_{sc}, V_{oc}, FF, Eff) of a solar cell structure made up of FTO/ETL/$CH_3NH_3PbI_3$/$CuInSe_2$/Au. Gold makes up the back contact, and tin oxide doped with fluorine (FTO) makes up the front contact. These two compounds have work roles are 5.47 eV and 4.4 eV respectively. Zinc oxide, both undoped and doped, makes up the electron transport layer, whereas methyl ammonium lead iodide makes up the absorber layer. Thin sheets, indium diselenide, and copper make up the hole transport layer. An optimal perovskite layer was obtained by decreasing the electron transportation layer's thickness (ETL) from 500 to 100 nm. For the In_ZnO ETL, this optimization was accomplished at 300K working temperature. Reduced ETL thickness was shown to result in higher efficiency (above 27%), as well as higher fill factor (above 87%). With a V_{oc} value of 1.180V, a FF value of 87.55%, and a J_{sc} value of 26.276mA/cm^2, the greatest efficiency performance of 27.15% was found. Using an absorber layer made of $CH_3NH_3PbI_3$ with a thickness of 800 nm and indium-doped oxide of zinc (In_ZnO) is the layer that transports electrons, this performance was achieved. The results are obtained at a constant irradiance level of 1000 W/m^2, under the AM1.5G spectrum.
Keywords: $CH_3NH_3PbI_3$. ZnO. SCAPS-1D. Carrier concentration. Thickness. Aluminum doped ZnO. Indium doped ZnO.

1. Introduction

Owing to its potential for applications requiring high-performance solar cells at a reasonable cost, perovskite organic-inorganic material has garnered significant interest when employed as an active element in solar cells [1]. This material is a good contender for next developments in solar cell technology because of its encouraging properties [2]. Copper indium diselenide is widely used in the fabrication of thin-film solar cells ($CuInSe_2$) and oxide of zinc (ZnO) as raw materials. In particular, ZnO is the layer responsible for transporting electrons, while $CuInSe_2$ is responsible for transporting holes in perovskite solar cells that use methylammonium lead iodide ($CH_3NH_3PbI_3$) as the active component [3,4].

The band gap that defines the material is about 1 eV [5] and 3.26 eV [6] and displays a direct energy transition because of its strong absorption coefficient (10E+5 cm^{-1}) [7,8]. Furthermore, the cheap cost of its production processes—such as electrodeposition, sol-gel, and spray pyrolysis—is a distinguishing feature. ZnO and $CuInSe_2$ are important materials when considering renewable energy and their applications [9]. The compound $CH_3NH_3PbI_3$ has a strong absorption coefficient (α) [10,11] and the gap in the band of the straight transition about of 1.66 eV [10]. It is therefore utilized as the active layer in p-i-n and n-i-p designs. The efficiency of solar cells that use methyl ammonium lead iodide has significantly increased recently [12,13], considering level of illumination of 1000 W/m^2.

Various metals can be doped into zinc oxide, including Indium, Gallium and Aluminium, to enhance its electrical, optical, and structural characteristics [14-17]. Oxide of Zinc (ZnO) thin transparent conductive films, both doped and undoped, are important for electrical and optical devices, particularly in the context of solar cells [15]. Here, we report the findings of a computerized model simulation of a solar cell that uses methylammonium. (MA) lead iodide as the active material. The simulations were conducted using a one-dimensional SCAPS-1D simulator. The photovoltaic cell structure's electron transportation layer (ETL), which is made up of FTO/ETL/$CH_3NH_3PbI_3$/$CuInSe_2$/Au, was composed of pure ZnO (P_ZnO), Indium doped ZnO (In_ZnO), and Aluminum doped ZnO (Al_ZnO). We investigated the effects of carrier concentration and thickness (W) depending on the solar cell's efficiency. The acquired data show a fill factor value greater than 87%.

2. Details of simulation

In this title, we employ $CuInSe_2$ as the hole transport layer (p-type), $CH_3NH_3PbI_3$ as the absorber layer (p-type), and undoped ZnO, aluminum-doped ZnO, and indium-doped ZnO as the electron transport layers (n-type). Furthermore, we utilize gold (Au) as a back contact for an analytical function of (ϕ) of 5.47 eV [18] and SnO_2: F (FTO) as the front contact with analytical function (ϕ) of 4.4 eV [19], so it is illustrated in Figure 1.

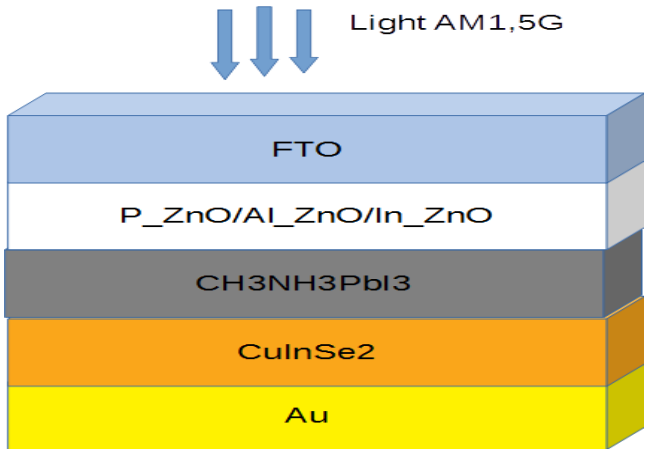

Figure1: representation of the structure of $CH_3NH_3PbI_3$ solar cell.

The Electronics and Information Systems Department (ELIS) at Gent University in Belgium is where the SCAPS program originated [1]. As mentioned earlier, the calculations are executed through the resolution of a trio of essential equations, specifically the formula for Poisson (equation 1) and the continuation formulas that regulate the conduct of holes and electrons. (equations 2 and 3) [20, 21].

$$\frac{d}{dx}\left(\varepsilon(x)\frac{d\psi}{dx}\right) = q[p(x) - n(x) + N_D^+(x) - N_A^-(x) + p_t(x) - n_t(x)] \quad (1)$$

$$\frac{1}{j}\frac{\partial J_p}{\partial x} + R_p(x) - G(x) = 0 \quad (2)$$

$$\frac{1}{j}\frac{\partial J_n}{\partial x} + R_n(x) - G(x) = 0 \quad (3)$$

Where:

- ε permittivity;
- ψ potential electrostatically.
- q charge of electron.
- n, p concentration of electrons and holes.
- n_t, p_t confined electron (negative charge), hole (positive charge).
- N_D^+, N_A^+ ionized doping concentration of donor and acceptor.
- $R_n(x)$, $R_p(x)$ electrons and holes recombination rates.
- G(x) generation rating.
- J_n and J_p electron and hole current densities.

All parameters of simulation are selected in table 1 from experimental and other theoretical results [2][4][6][9][22–26], the absorption coefficient (α) of CH3NH3PbI3 prepared by [2], while the absorption coefficient of ZnO and CuInSe2 by SCAPS 1d.

Table1– The simulation parameters of the input file on the $CH_3NH_3PbI_3$ solar cell.

	P_ZnO	Al_ZnO	In_ZnO	$CH_3NH_3PbI_3$	$CuInSe_2$
W (nm)	**100-500**	**100-500**	**100-500**	800	200
Eg (eV)	3.26	3.269	3.28	1.54	1.07
ξ_r	9	9	9	6.5	9
X_e (eV)	4.1	4.1	4.1	3.93	4
μ_n (cm²/Vs)	100	100	100	2	5.000×10^{-4}
μ_p (cm²/Vs)	25	25	25	2	5.000×10^{-4}
N_c (1/cm³)	2.22×10^{18}	2.22×10^{18}	2.22×10^{18}	2.2×10^{18}	2.2×10^{18}
N_v(1/cm³)	1.8×10^{19}	1.8×10^{19}	1.8×10^{19}	1.8×10^{19}	1.8×10^{19}
N_d (1/cm³)	2×10^{13}	7.589×10^{18}	1.2×10^{20}	0	0
N_a (1/cm³)	0	0	0	2×10^{17}	2×10^{16}
Vth_e(cm/s)	1×10^{7}	1×10^{7}	1×10^{7}	1×10^{6}	1×10^{7}
Vth_h (cm/s)	1×10^{7}	1×10^{7}	1×10^{7}	1×10^{6}	1×10^{7}

3. Results and discussions

3.1 *Effect of carrier concentration of ETL on $CH_3NH_3PbI_3$ cells*

In the following subsection, we examine the zinc oxide's N_d doped percentage concentration, we use undoped ZnO (P_ZnO), Aluminum doped ZnO (Al_ZnO) and Indium doped ZnO (In_ZnO) in this structure "FTO/ (P_ZnO, Al_ZnO, In_ZnO)/$CH_3NH_3PbI_3$/$CuInSe_2$/Au".

Undoped ZnO prepared by S.Benzitouni et al in 2018 [6], the obtained result 3.26eV as band gap energy (Eg) and carrier concentration (N_d) equal to 2*10^13cm^{-3}. The Al doped ZnO prepared by A.Nakrela and co-authors [22], he obtained 3.269eV as band gap energy and the N_d equal to 7.589×10^{18} cm^{-3}. The In doped ZnO prepared in 2014 by [23], he obtained 3.28eV as Eg and the N_d equal to 1.2×10^{20} cm^{-3}(Table 2).

Table2 - cell performances on perovskite solar cell.

Structure	N_d (cm^{-3})	Eg (eV)	W (nm)	Eff (%)	FF (%)	J_{sc} (mA/cm^2)	V_{oc} (V)
P_ZnO/$CH_3NH_3PbI_3$/$CuInSe_2$	2×10^{13}	3.26	488	25.43	83.81	25.723	1.179
Al_ZnO/ $CH_3NH_3PbI_3$/$CuInSe_2$	7.589×10^{18}	3.269	100	27.02	87.25	26.244	1.180
In_ZnO/ $CH_3NH_3PbI_3$/$CuInSe_2$	1.2×10^{20}	3.28	197	26.90	87.55	26.037	1.179

The impact of the concentration of transporters N_d of P_ZnO, Al_ZnO, and In_ZnO with thickness (W) and band gap (Eg) variables was prepared by experimental results (see table 2). N_d was varied from 2×10^{13} to 1.2×10^{20} cm^{-3}. The efficiency increased from 25.43 to 27.02% as well as the same the fill factor (FF) coming from 83.81 to 87.55%.

Table 2 presents the data illustrating the fluctuations in carrier concentration (N_d) under short-circuit conditions. The current density at short circuit (J_{SC}) and the open circuit voltage (V_{oc}) were investigated in this study. It was shown that J_{sc} rose from 25.723mA/cm^2 for P_ZnO to 26.244mA/cm^2 for Al-doped ZnO, while it reduced to 26.037mA/cm^2 for indium-doped ZnO. However, the change in V_{oc} was found to be minor. The decrease in resistivity with increased ETL doping concentration can be attributed to this phenomenon [27].

In an investigation led by Adhikari and al. in 2016, the researchers investigated the impact of the dopant concentration of electron transport materials (ETMs) about the efficiency of solar cells. The results of their study indicated that the spiroMeOTAD/$MAPbI_3$/ZnO structure achieved an efficiency of 22.49% [28]. The incorporation of aluminum (Al) and indium (In) into zinc oxide (ZnO) results in highly favorable perovskite solar cell characteristics, specifically yielding a maximum fill factor value above 87%.

3.2 Role of thickness for each case on cell performance

The thickness (W) of doped and undoped ZnO varied from 100 to 500nm, while keeping the absorber ($CH_3NH_3PbI_3$) and HTL ($CuInSe_2$) layer thickness at 800 and 200nm respectively.

Figure 2 Clarifies the connection between $CH_3NH_3PbI_3$ solar cells' performance and the ETL layer thickness. It is observed that the efficiency experiences a minor decline from 26.08% to 25.41%, 27.02% to 26.43%, and 27.15% to 26.54% for P_ZnO, Al_ZnO, and In_ZnO, respectively. The fill factor experiences a reduction from 84.53% to 83.77% in the case of P_ZnO. However, in the case of Al_ZnO, it was observed that the fill factor (FF) exhibited a little rise from 87.25% to 87.28% with the electron transport layer (ETL) the thickness of was increased (Figure 3). The effects involve altering the electron transport layer's thickness (ETL), namely In_ZnO and Al_ZnO, on the fill factor (FF) is negligible. The J_{sc} values for P_ZnO, Al_ZnO, and In_ZnO structures (Figure 4) fall from 26.144 to 25.719 mA/cm^2, 26.244 to 25.664mA/cm^2, and 26.276 to 25.694mA/cm^2, respectively. Conversely, the V_{oc} values (Figure 5) exhibit negligible changes. Each outcome aligns with the study carried out by Jayakumar et al [29] and Aseena et al [30].

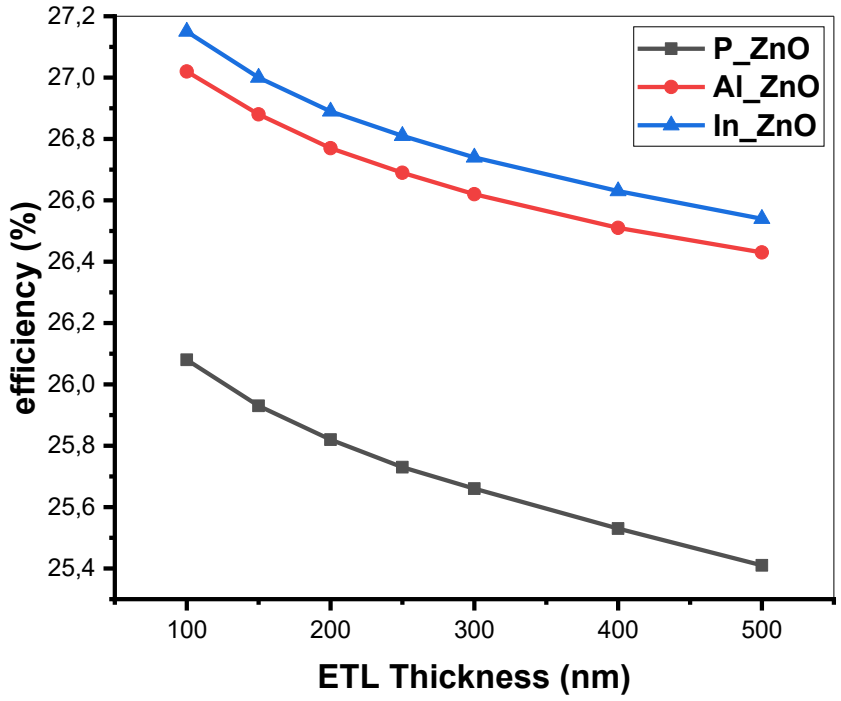

Figure 2: influence of thickness for each case on efficiency.

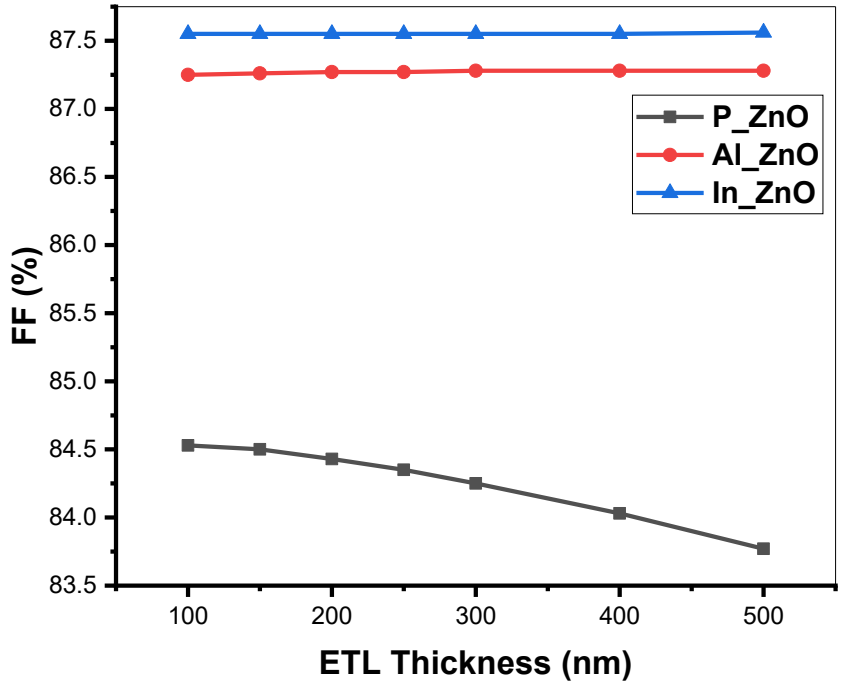

Figure 3: influence of thickness for each case on fill factor.

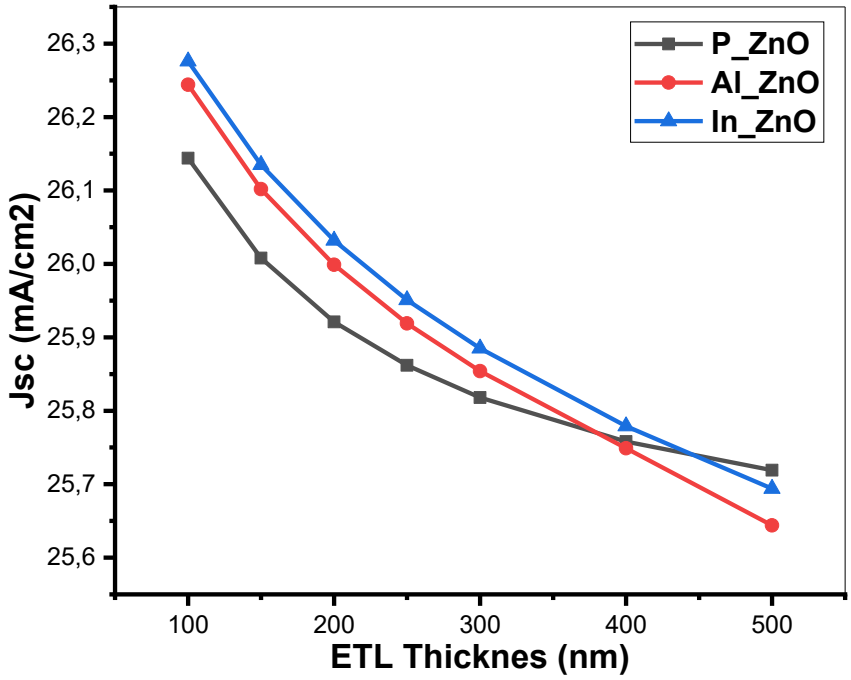

Figure 4: influence of thickness for each case on short circuit current density (J_{sc}).

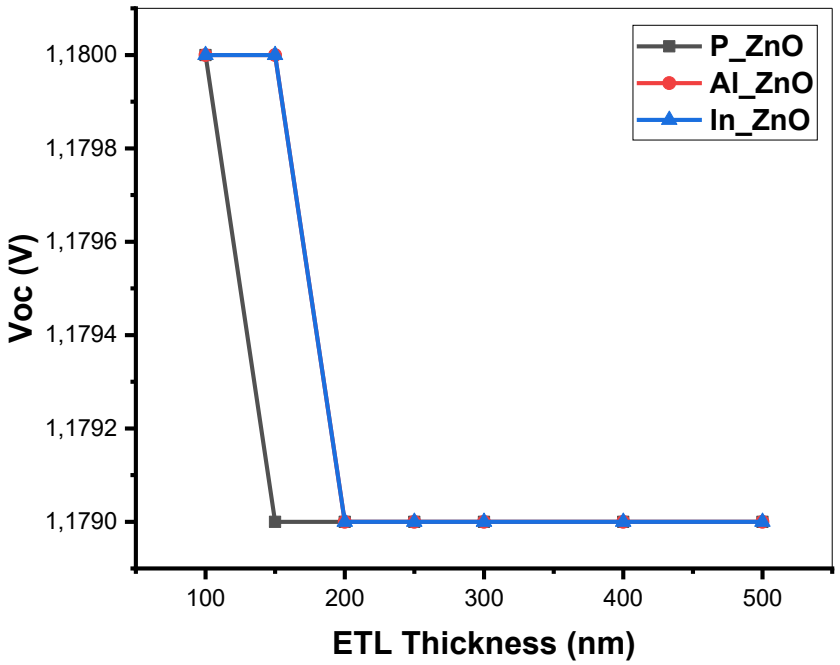

Figure 5: Influence of thickness for each case on open circuit voltage.

The optimized layer thickness of ETL is 100nm which corresponds to a maximum efficiency of 26.08%, 27.02% and 27.15% for P_ZnO, Al_ZnO and In_ZnO respectively.

4. J-V Characteristic and quantum efficiency

Table 1 shows the preset doping density, absorber thickness, and hole transport layer (HTL) thickness. However, the electron transport layer's (ETL) thickness is fixed at 100 nm in each situation. Each of the three structures J-V properties, namely P_ZnO, Al_ZnO, and In_ZnO/$CH_3NH_3PbI_3$/$CuInSe_2$, exhibit a high degree of similarity, as seen in Figure 6. Figure 7 demonstrates the quantum efficiency, indicating that opting for a broader energy gap for the electron transport layer (ETL) results in a notable enhancement in photon absorption within the ultraviolet (UV) spectrum [31].

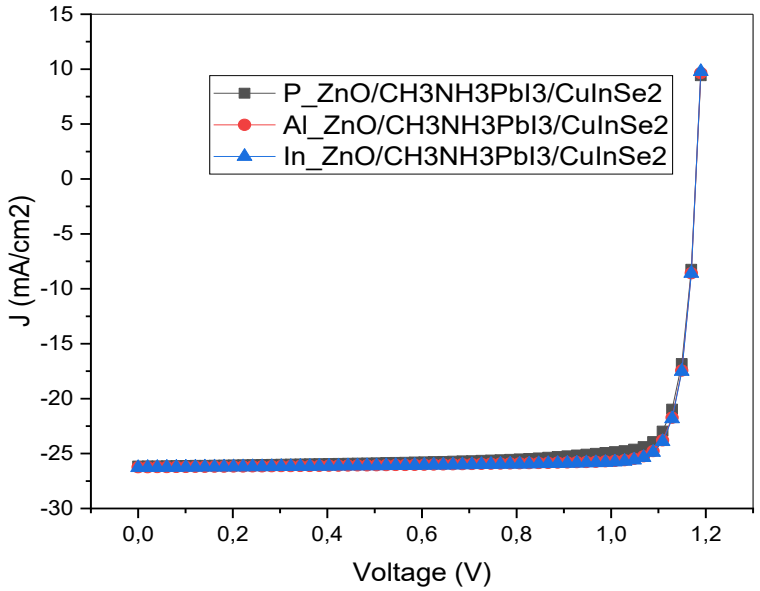

Figure 6: (P_ZnO, Al_ZnO, In_ZnO) as ETLs J-V characteristics

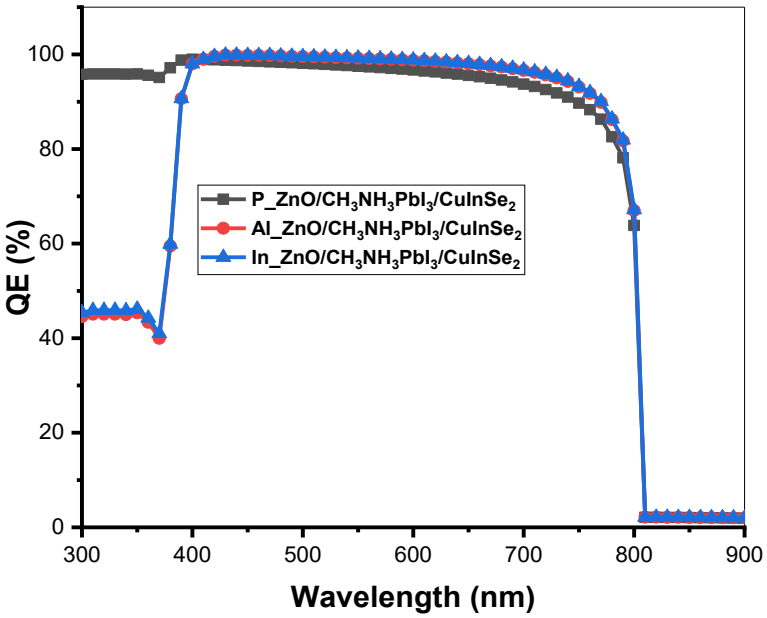

Figure 7 : $CH_3NH_3PbI_3$ solar cell quantum efficiency (QE)

5. Conclusions

The main object of this study is to find out what the transport layer of electron (ETL) does for the structure of a $CH_3NH_3PbI_3$ solar cell that uses P_ZnO, Al_ZnO, and In_ZnO as electron transport materials (ETMs). We explore the influence of carrier concentration N_d and thickness (w) of ETMs on cell performances. Al and In-doped ZnO offer good perovskite solar cell characteristics, but there is a little variation in findings between doping with Al and In. A statistical examination was conducted to compare the efficiency of devices and the level of quality of the perovskite layer. When we assess, there is a significant enhancement observed in the steady-state Fill factor to 87.55% and efficiency equal to 27.15%.

References

[1] U. Mandadapu, S. V. Vedanayakam, K. Thyagarajan, M. R. Reddy and B. J. Babu,(2017), Design and Simulation of High Efficiency Tin Halide Perovskite Solar Cell, no. December, Int. J. Renew. Energy Res, 7(4), 1604-1612.

[2] S. Wang, K. Zhao, Y. Shao, L. Xu, Y. Huang and W. Li, (2020), Evolutions of optical constants , interband electron transitions , and bandgap of Sn- doped $CH_3NH_3PbI_3$ perovskite films, *Appl. Phys. Lett.*, vol. 261902, no. March, doi: 10.1063/5.0007293.

[3] M. A. Zaman, M. Akhtaruzzaman and M. J. Rashid,(2019), Influence of Electron Transport Layer on the Performance of Perovskite Solar Cell, *ICIET 2019 - 2nd Int. Conf. Innov. Eng. Technol.*, pp. 23–24, doi: 10.1109/ICIET48527.2019.9290690.

[4] Gagandeep, M. Singh, R. Kumar and V. Singh,(2021), Investigation of $CH_3NH_3PbI_3$ and $CH_3NH_3SnI_3$ based perovskite solar cells with $CuInSe_2$ nanocrystals, *Optik (Stuttg).*, vol. 246, no. January, p. 167839, doi: 10.1016/j.ijleo.2021.167839.

[5] A.E. Zaghi, M. Buffiere, G. Brammertz, N. Lenaers, M. Meuris, J. Poortmans and J. Vleugels, (2014), Selenization of printed Cu-In-Se alloy nanopowder layers for fabrication of $CuInSe_2$ thin film solar cells, *Thin Solid Films*, doi: 10.1016/j.tsf.2014.10.038.

[6] S. Benzitouni, M. Zaabat, A. Mahdjoub, A. Benaboud and B. Boudine, (2018), High transparency and conductivity of heavily In-doped ZnO thin films deposited by dip-coating method, *Mater. Sci.*, vol. 36, no. 3, pp. 427–434.

[7] A. Bouich, S. Ullah, H. Ullah, B. Mari, M. Ebn Touhami, B. Hartiti and D. M.F.Santos,(2018), Optoelectronic Characterization of CuIn (S , Se)$_2$ Thin Grown by Spray Pyrolysis Method for Solar Cells, pp.2–6, doi: 10.1109/IRSEC.2018.8702992.

[8] K. Adaikalam, S. Valanarasu, A. M. Ali, M. A. Sayed, W. Yang and H. Kim, (2022),Photosensing effect of indium-doped ZnO thin films and its heterostructure with silicon, *J. Asian Ceram. Soc.*, vol. 10, no. 1, pp. 108–119, doi: 10.1080/21870764.2021.2015847.

[9] J. Shi, Y. Chen, C. Chen and P. Wu,(2012), Optical properties and synthesis of $CuInSe_2$ thin films by selenization of Cu / In layers, *Cryst. Res. Technol.*, vol. 186, no. 2, pp. 183–186, doi: 10.1002/crat.201100529.

[10] D. Liu, X. Li, C. Shi and Q. Liang,(2016), $CH_3NH_3PbI_3$ thin films prepared by pulsed laser deposition for optoelectronic applications, *Mater. Lett.*, doi: 10.1016/j.matlet.2016.10.113.

[11] M. Girtan, (2020), On the electrical and photoelectrical properties of $CH_3NH_3PBI_3$ perovskites thin films, *Sol. Energy*, vol. 195, no. September 2019, pp. 446–453, doi: 10.1016/j.solener.2019.11.096.

[12] I. Montoya De Los Santos, H. J. Cortina-Marrero, M.A. Ruíz-Sánchez, L. Hechavarría-Difur, F.J. Sánchez-Rodríguez, M. Courel and H. Hu,(2020), Optimization of $CH_3NH_3PbI_3$ perovskite solar cells: A theoretical and experimental study, *Sol. Energy*, vol. 199, no. November 2019, pp. 198–205, doi: 10.1016/j.solener.2020.02.026.

[13] J. Zhang, X. Li, L. Wang, J. Yu, S. Wageh and A. A. Al-ghamdi,(2021), Applied Surface Science Enhanced performance of CH $_3$ NH $_3$ PbI $_3$ perovskite solar cells by excess halide modification, *Appl. Surf. Sci.*, vol. 564, no. June, p. 150464, doi: 10.1016/j.apsusc.2021.150464.

[14] M. Benhaliliba, C. E. Benouis, M. S. Aida, F. Yakuphanoglu and A. S. Juarez,(2010), Indium and aluminium-doped ZnO thin films deposited onto FTO substrates : nanostructure , optical , photoluminescence and electrical properties, *J Sol-Gel Sci Technol*, pp. 335–342, doi: 10.1007/s10971-010-2258-x.

[15] M. U. Shahid, K. M. Deen, A. Ahmad, M. A. Akram, M. Aslam and W. Akhtar,(2016), Formation of Al-doped ZnO thin films on glass by sol – gel process and characterization, *Appl. Nanosci.*, pp. 235–241, doi: 10.1007/s13204-015-0425-7.

[16] S. P. Bharath, K. V Bangera and G. K. Shivakumar,(2018), Enhanced gas sensing properties of indium doped ZnO thin films, *Superlattices Microstruct.*, doi: 10.1016/j.spmi.2018.10.010.

[17] Y. Nishi, Y. Kasai, R. Suzuki, M. Matsubara, A. Muramatsu and K. Kanie,(2020), Gallium-Doped Zinc Oxide Nanoparticle Thin Films as Transparent Electrode Materials with High Conductivity, *ACS Appl. Nano Mater*, doi: 10.1021/acsanm.0c01471.

[18] J. P. M. Serbena, K. D. Machado, M. C. Siqueira, I. A. Hummelgen, R. J. O. Mossanek, G. B. de Souza and J. H. D. da Silva, (2014), SeP hole injection layer for devices based on organic materials, *J. Phys. D Appl. Physic*, vol. 47, no. 015304, p. 6pp, doi: 10.1088/0022-3727/47/1/015304.

[19] H. B. Michaelson, (1977), The work function of the elements and its periodicity, *J. Appl. Phys.*, vol. 48, no. 11, pp. 4729–4733, doi: 10.1063/1.323539.

[20] S. Rai, B. K. Pandey and D. K. Dwivedi,(2020), Modeling of highly efficient and low cost CH_3NH_3 Pb(I_{1-x} Cl_x)$_3$ based perovskite solar cell by numerical simulation, *Opt. Mater. (Amst).*, vol. 100, no. October 2019, doi: 10.1016/j.optmat.2019.109631.

[21] K. Bhavsar and P. B. Lapsiwala, (2021), Optoelectronics and optoelectronic devices Numerical simulation of perovskite solar cell with different material as electron transport layer using SCAPS-1D software,*Semicond. Physics, Quantum Electron. Optoelectron.*, vol. 24, no. 3, pp. 341–347.

[22] A. Nakrela, N. Benramdane, A. Bouzidi, Z. Kebbab, M. Medles and C. Mathieu, (2016), Site location of Al-dopant in ZnO lattice by exploiting the structural and optical characterisation of ZnO : Al thin films, *Results Phys.*, vol. 6, pp. 133–138, doi: 10.1016/j.rinp.2016.01.010.

[23] R. Bel-hadj-tahar and A. B. Mohamed, (2014),Sol-Gel Processed Indium-Doped Zinc Oxide Thin Films and Their Electrical and Optical Properties, no. October, pp. 55–65.

[24] A. coulibaly, A. Bouich, Sh.ullah and N.G. Kre, (2020), Experimental and Numerical study of ($CH_3NH_3PbI_3$) $MaPbI_3$ thin film with fluorene- dithiophene (FDT) or spiroometad as hole transporter layer, vol. 12, no. 2, pp. 17–26, doi: 10.9790/4861-1202021726.

[25] D. A. Fentahun, A. Tyagi and K. K. Kar,(2021), Numerically investigating the AZO / Cu_2O heterojunction solar cell using ZnO / CdS buffer layer, *Optik (Stuttg).*, vol. 228, no. May 2020, p. 166228, doi: 10.1016/j.ijleo.2020.166228.

[26] Q. Zhou , D. Jiao , K. Fu , X. Wu, Y. Chen, J. Lu and S. Yang, (2016), Two-dimensional device modeling of $CH_3NH_3PbI_3$ based planar heterojunction perovskite solar cells, *Sol. Energy*, vol. 123, pp. 51–56, doi: 10.1016/j.solener.2015.11.009.

[27] P. Zhao, Z. Liu, Z. Lin, D. Chen, J. Su, Ch. Zhang, J. Zhang, J. Chang and Y. Hao, (2018), Device simulation of inverted $CH_3NH_3PbI_{3-x}Cl_x$ perovskite solar cells based on PCBM electron transport layer and NiO hole transport layer, *Sol. Energy*, vol. 169, no. April, pp. 11–18, doi: 10.1016/j.solener.2018.04.027.

[28] K. R. Adhikari, S. Gurung, B. K. Bhattarai and B. M. Soucase,(2016), Comparative study on $MAPbI_3$ based solar cells using different electron transporting materials, *Phys. Status Solidi Curr. Top. Solid State Phys.*, vol. 13, no. 1, pp. 13–17, doi: 10.1002/pssc.201510078.

[29] R. Jeyakumar, A. Bag, R. Nekovei and R. Radhakrishnan, (2020), Influence of Electron Transport Layer (TiO_2) Thickness and Its Doping Density on the Performance of $CH_3NH_3PbI_3$-Based Planar Perovskite Solar Cells, *J. Electron. Mater.*, vol. 49, no. 6, pp. 3533–3539, doi: 10.1007/s11664-020-08041-w.

[30] S. Aseena, N. Abraham and V. Suresh Babu, (2020), Optimization of layer thickness of ZnO based perovskite solar cells using SCAPS 1D, *Mater. Today Proc.*, vol. 43, pp. 3432–3437,

doi: 10.1016/j.matpr.2020.09.077.

[31] N. Gamal, S. H. Sedky, A. Shaker and M. Fedawy, (2021), Design of lead-free perovskite solar cell using $Zn_{1-x}Mg_xO$ as ETL : SCAPS device simulation, *Optik (Stuttg).*, vol. 242, no. May, p. 167306, doi: 10.1016/j.ijleo.2021.167306.